Structural Changes at the Metal Ion Binding Site during the Phosphoglucomutase Reaction†

William J. Ray, Jr.,*,‡ Carol Beth Post,§ Y. Liu,‡ and Gyung Ihm Rhyu‡,∥

Appendix: NMR Line Shape Analysis and Enzyme Binding

Carol Beth Post§

Departments of Biological Sciences and Medicinal Chemistry, Purdue University, West Lafayette, Indiana 47907

Received April 21, 1992; Revised Manuscript Received August 25, 1992

ABSTRACT: An electron density map of the reactive, Cd^{2+} form of crystalline phosphoglucomutase from X-ray diffraction studies shows that the enzymic phosphate donates a nonbridging oxygen to the ligand sphere of the bound metal ion, which appears to be tetracoordinate. ^{31}P and ^{113}Cd NMR spectroscopy are used to assess changes in the properties of bound Cd^{2+} produced by substrate/product and by substrate/product analog inhibitors. The approximately 50 ppm downfield shift of the ^{113}Cd resonance on formation of the complex of dephosphoenzyme and glucose 1,6-bisphosphate is associated with the initial sugar–phosphate binding step and likely involves a change in the geometry of the coordinating ligands. This interpretation is supported by spectral studies involving various complexes of the active Co^{2+} and Ni^{2+}–enzyme. In addition, there is a loss of the ^{31}P–^{113}Cd J coupling that characterizes the monophosphate complexes of the Cd^{2+} enzyme either during or immediately after the PO_3^- transfer step that produces the bisphosphate complex, indicating a further change at the metal binding site. The implications of these observations with respect to the PO_3^- transfer process in the phosphoglucomutase reaction are considered. The apparent plasticity of the ligand sphere of the active site metal ion in this system may allow a single metal ion to act as a chaperone for a nonbridging oxygen during PO_3^- transfer or to allow a change in metal ion coordination *during* catalysis. A general NMR line shape/chemical-exchange analysis for evaluating binding in protein–ligand systems when exchange is intermediate to fast on the NMR time scale is described. Its application to the present system involves multiple exchange sites that depend on a single binding rate, thereby adding further constraints to the analysis.

When the phospho form of phosphoglucomutase, E_P,[1] is treated with an equilibrium mixture of Glc-1-P and Glc-6-P in the presence of an activating metal ion, M, a mixture of complexes is produced: E_P(M)Glc-1-P + E_P(M)Glc-6-P + E_D(M)Glc-1,6-P_2 (Ray & Long, 1976a). When M = Cd^{2+}, the equilibrium among these complexes shifts so that E_D-(Cd)Glc-1,6-P_2 predominates by about 10:1 (Ray & Long, 1976b). Thus, the bisphosphate complex can be studied in the essential absence of monophosphate complexes.

An earlier ^{31}P NMR study employing ^{113}Cd (Rhyu et al., 1984) showed that in the binary E_P(Cd) complex the enzymic phosphate group coordinates directly with the bound metal ion: $J_{CdP} \approx 16$ Hz. This and two related studies (Rhyu et al., 1985a,b) documented three changes that accompany the conversion of E_P(Cd) into the E_D(Cd)Glc-1,6-P_2 complex: the ^{31}P–^{113}Cd coupling becomes undetectable, the ^{113}Cd resonance shifts downfield by about 50 ppm, and a histidine side chain that titrates normally in E_P(Cd) no longer can be deprotonated at relatively high pH. Although there was no compelling reason to link these observations, a possible coupling was suggested because of its simplicity.

The current study was initiated to test the above coupling by examining the changes produced by a process analogous to the first step of the two-step conversion of E_P(Cd) into E_D(Cd)Glc-1,6-P_2: the substrate-binding step. Because of the relatively high effective chemical potential of the enzymic phosphate group in the E_P(Cd)Glc-P complexes (Ray & Long, 1976b), as well as the catalytic competence of these and related sugar phosphate complexes, no sugar phosphate with an appropriately positioned acceptor hydroxyl group can be used in a simple binding study; otherwise the binding step will be followed by PO_3^- transfer[2] before properties of the initial complex can be assessed, even with a poor substrate. Hence, we employ the deoxysugar phosphate inhibitors related to Glc-1-P and Glc-6-P: 6-dGlc-1-P and 1-dGlc-6-P, respectively. Although in the present system these dGlc-P inhibitors bind somewhat weaker and somewhat stronger, respectively, than do their reactive counterparts, on binding both produce a characteristic substrate-induced or product-induced UV difference spectrum (Ma & Ray, 1980). Thus, both apparently induce the same or nearly the same conformational changes as do the corresponding glucose phosphates.

† This work was supported in part by a research grant from the U.S. Public Health Service (GM08963, to W.J.R.), a grant from the Biotechnology Resources Program of the Division of Research Resources, National Institutes of Health (RR01077, to the Purdue University Biochemical Magnetic Resources Laboratory), grants from the NSF Biological Instrumentation Division (8714248 and BMS8614177, to the Purdue Biological Facilities Center on Biomolecular NMR, Structure and Design), and a grant from the Lucille P. Markey Charitable Trust.

* To whom correspondence should be addressed.

‡ Department of Biological Sciences.

§ Department of Medicinal Chemistry.

∥ Present address: Organic Chemistry Research Center, Sogang University, 1 Shinsu-dong, Mapo-ku, Seoul, Korea.

[1] Abbreviations: Glc-1-P, α-D-glucose 1-phosphate; Glc-6-P, glucose 6-phosphate, in solution, a mixture of α- and β-anomers, in complexes with phosphoglucomutase in the α-anomer is implied; Glc-1,6-P_2 or Glc-P_2, α-D-glucose 1,6-bisphosphate; 6-dGlc-1-P, α-D-gluco-1,5-anhydro-6-deoxyglucose 1-phosphate or 6-deoxyglucose 1-phosphate; 1-dGlc-6-P, D-gluco-1,5-anhydrohexitol 6-phosphate or 1-deoxyglucose 6-phosphate; dGlc-P, a mixture of 6-dGlc-1-P and 1-dGlc-6-P; Ac, acetate; E_P and E_D, the phospho and dephospho forms, respectively, of phosphoglucomutase; M, a bivalent metal ion; ΣE(M)Glc-P, an equilibrium mixture of the catalytically active, central complexes; F, structure factor.

[2] PO_3^- transfer refers to stoichiometry, not mechanism.

0006-2960/93/0432-48$04.00/0

In the present study, we examine the Cd^{2+}, Co^{2+}, and Ni^{2+} complexes of the enzyme, although the Mg^{2+} complex is the physiologically active form of the enzyme and exhibits maximal activity. However, all four metal ions increase k_{cat} by many orders of magnitude, relative to the metal-free enzyme (Ray, 1969; Ray et al., 1989), without substantially affecting substrate binding (Ray & Long, 1976b), and k_{cat} for the Ni^{2+} enzyme is almost 0.75 that for the Mg^{2+} enzyme. In addition, the Cd^{2+} enzyme, which is the least active of these forms of the enzyme in terms of k_{cat} (0.01% that of the Mg^{2+} enzyme), is almost as good a catalyst as the Mg^{2+} enzyme in terms of k_{cat}/K_m (W.J.R., unpublished results) and is about 20% as efficient in terms of rate constant for the first PO_3^- transfer step (Ray et al., 1989).

Since this study is directed primarily toward complexes with the stoichiometry phosphoenzyme, metal ion, and glucose phosphate, we emphasize the fact that the binding of *one and only one* metal ion produces maximal enzymic activity [tested metal ions: Cd^{2+} (W.J.R., unpublished results), Co^{2+}, Mn^{2+}, Zn^{2+} (Ray, 1969), and Ni^{2+} (Ray et al., 1972)], although ancillary metal ion binding sites have been detected for Cd^{2+} (Rhyu et al., 1985a) Co^{2+}, Mn^{2+}, Ni^{2+} (Ray et al., 1972; Ray & Mildvan, 1970), and Li^+ (Rhyu et al., 1985a).

EXPERIMENTAL PROCEDURES

The synthesis of the deoxysugar phosphates has been described (Ma & Ray, 1980). ^1H, ^{31}P, and ^{113}Cd NMR studies were conducted as in Rhyu et al. (1984, 1985a,b). Line shape simulations of ^{31}P NMR spectra are described in the Appendix. The phospho form of phosphoglucomutase [M_R = 61 600 (Ray et al., 1983)] was prepared and freed from contaminating metal ions by unpublished procedures that are available on request. In general, absorption spectra were obtained as in Ray et al. (1990) (see also the figure legends).

Mg(II) and Cd(II) Complexes of the Crystalline Phosphoenzyme. Diffraction grade crystals of phosphoglucomutase (Dai et al., 1992) that were largely in the dephospho form were treated with Glc-P_2 to produce the crystalline E_P(Mg) complex (Ray & Puvathingal, 1991). To obtain the Cd^{2+} complex, the concentration of Mg^{2+}/EDTA in "storage buffer" was reduced from 16 mM/1 mM to 1 mM/0.5 mM in five steps (see above reference). Three additional steps were used to transfer the crystals to same buffer that contained 2 mM $CdAc_2$ instead of Mg^{2+}/EDTA. The $CdAc_2$ solution was replaced several times over a period of 24 h. Multiturnover end-point assays of crystals crushed in the presence of excess substrate and EDTA [cf. Magneson et al. (1986) and Ray and Puvathingal (1991)] were used to monitor the replacement of Mg^{2+} by Cd^{2+}: $\tau_{1/2}$ about 0.5 h for millimeter-size crystals.

X-ray Diffraction Studies. Diffraction data for E_P(Mg) and E_P(Cd) were collected by using a SDMW (Hamlin) two-chamber area detector system mounted on a Regaku AFC-6 four-circle diffractometer, powered by a Regaku rotating anode X-ray generator. The 2θ value was 10° and 25° and the frame size 0.1° (collection time was 1 min per frame) so that reciprocal space was covered to 2.6-Å resolution using two crystals per data set. The energy minimization procedure of X-PLOR (Brunger et al., 1989) was used to fit the previously refined model of the metal-free dephosphoenzyme (Dai et al., 1992) to the processed reflections where $F/\sigma \geq 2$, after attaching a PO_3 group to $Ser^{116}O\gamma$ and adding a metal "ion", based on density in the appropriate difference maps. (Because of the complex electrostatic interactions in this region of the molecule and the uncertain location of formal charges, the refinement was conducted with electrically neutral groups, including Cd^0 and Mg^0. This means that the position of atoms in the model is determined primarily by van der Waals interactions and the X-ray energy term of X-PLOR.) Electron density maps ($2F_o - F_c$) were constructed by using the processed data plus structure factors and phases calculated from the model and were displayed, along with the model, on a computer graphics system by using the interactive program FRODO (Jones, 1978).

RESULTS

Deoxyglucose Phosphate Complexes of the Cd(II) Enzyme: ^{31}P and ^{113}Cd NMR Studies. Figure 1 shows the effect of added dGlc-6-P on the ^{31}P NMR spectrum of a solution that contains E_P plus excess $^{113}CdAc_2$ (1.5 equiv total), since to saturate the metal binding site with Cd^{2+}, one must partially saturate an ancillary site [W.J.R., unpublished results; see also Rhyu et al. (1985a)]. In Figure 1a the partial splitting of the ^{31}P resonance of the phosphoenzyme is caused by J coupling of ^{31}P and the $^{113}Cd^{2+}$ bound at the active site of the enzyme (Rhyu et al., 1985a). On addition of 0.64 enzyme equivalents of 1-dGlc-6-P (Figure 1b), the intensity of the ^{31}P doublet representing the enzymic phosphorus is partitioned between two resonances, one at ~3.7 ppm, which remains a doublet, and the other, an exchange-broadened resonance, at ~2.7 ppm. With further addition of 1-dGlc-6-P [Figure 1, panels c (0.96 equiv) and d (1.28 equiv)], the broadened enzymic resonance narrows and shifts to the same frequency as the doublet in Figure 1b, ~3.7 ppm. The J value for the enzymic phosphorus in both deoxyglucose phosphate complexes is approximately the same and does not differ significantly from that for E_P(Cd). On addition of excess 1-dGlc-6-P (Figure 1d), the deoxysugar phosphate resonance (at –0.8 ppm; Figure 1b) also shifts toward that of 1-dGlc-6-P (Figure 1a), accompanied by exchange broadening.

To define the exchange process giving rise to the spectra in Figure 1, the observed line shapes were modeled by using the equilibria in eqs 1 and 2 (after examining a variety of

$$\begin{array}{ccc} Cd^{2+} & & \\ + & & \\ Ep(Cd) + 1\text{-dGlc-6-P} & \rightleftharpoons & Ep(Cd)1\text{-dGlc-6-P} \quad (1) \\ \Updownarrow & & \\ Ep(Cd)_2 + 1\text{-dGlc-1-P} & \rightleftharpoons & Ep(Cd)1\text{-dGlc-6-P(Cd)} \quad (2) \end{array}$$

others). All reasonable simulations require that the binding of 1-dGlc-6-P to $E_P(Cd)_2$, where both active and ancillary sites are occupied, be somewhat tighter than to E_P(Cd), where only the active site is occupied. A slower dissociation of 1-dGlc-6-P from the E_P(Cd)1-dGlc-6-P(Cd) complex than from the corresponding mono-Cd complex also is required. Both requirements are in accord with observations made with other metal ion forms of the enzyme (W.J.R., unpublished results). The results of these spectral simulations, where the ^{31}P–^{113}Cd coupling was omitted, are shown in Figure 2. The binding of 1-dGlc-6-P to Ep(Cd) and the exchange between E_P(Cd) and $E_P(Cd)_2$ thus account reasonably well for the broadening and frequency shifts in Figure 1, especially since the observed spectra were obtained with a recycle time too short to allow full relaxation between scans, which differentially alters the observed intensities.

Results similar to those in Figure 1 also were obtained in an analogous titration of [E_P(Cd) + $E_P(Cd)_2$] with the more loosely bound 6-dGlc-1-P (not shown; cf. the chemical shifts

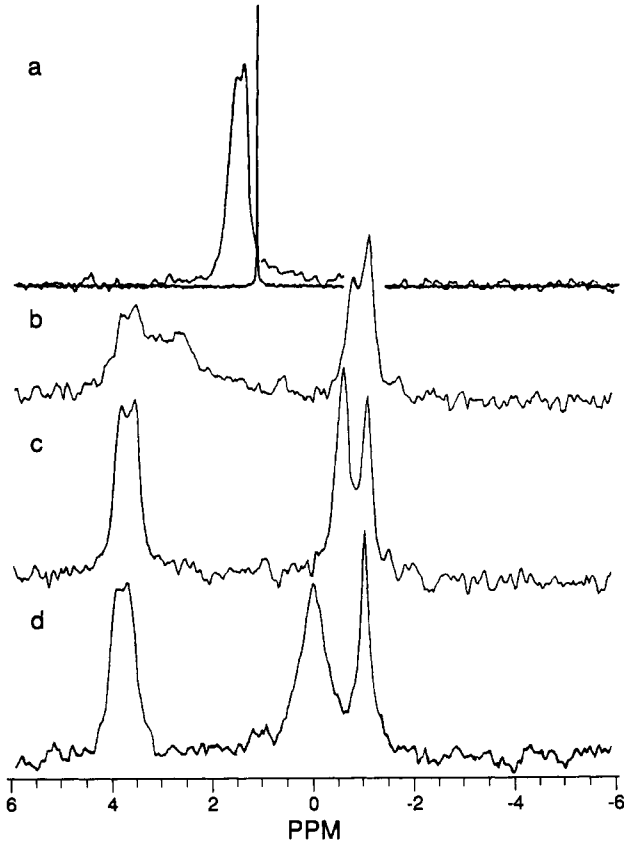

FIGURE 1: ^{31}P NMR spectroscopy of the ^{113}Cd complex of the phospho form of phosphoglucomutase in the presence of varying concentrations of 1-deoxyglucose 6-phosphate. The ^{113}Cd complex of the phosphoenzyme, $E_P(Cd)$, was obtained by the addition of 1.5 equiv of $^{113}CdAc_2$ to a solution of the metal-free phosphoenzyme: final enzyme concentration, 1.3 mM, in 20 mM Tris-HCl, pH 7.5, that contained 10% D_2O. Spectra [$T_1 \approx 5$ s (Post et al., 1989)] were measured with a 4.2-s recycle time, a 60° pulse angle, and 4096 transients at a 80.1-MHz field for ^{31}P. A line broadening factor of 5 Hz was applied before Fourier transformation as in Rhyu et al. (1984). Chemical shifts refer to trimethylphosphate. (a) Superimposed spectra of $E_P(^{113}Cd)$, the broad, split peak, and free 1-dGlc-6-P. (b–d) Spectra produced after addition of small volumes containing 0.64, 0.98, and 1.28 equiv of 1-dGlc-6-P, respectively.

in Table II of the accompanying paper).[3] Thus, the ^{113}Cd–^{31}P interaction that characterizes the binary $E_P(Cd)$ complex is retained in both ternary complexes of the deoxysugar phosphates.

Figure 3, top, shows ^{113}Cd NMR spectra of the catalytically active $E_D(Cd)Glc\text{-}P_2$ complex; Figure 3, middle and bottom, shows analogous spectra for the complexes of [$E_P(Cd)$ + $E_P(Cd)_2$] with 1-dGlc-6-P and 6-dGlc-1-P, respectively. The arrow, top spectrum, designates the chemical shift of ^{113}Cd in $E_P(Cd)$ prior to formation of the various sugar phosphate complexes. [The ancillary Cd^{2+} in $E_P(Cd_2)$ does not produce an NMR signal nor does it affect the chemical shift of the active site Cd^{2+} when it binds to Ep(Cd) (Rhyu et al., 1985a).] The minor upfield resonance in the presence of saturating dGlc-P (Figure 3, top and middle) apparently derives from the Cd_2 complex, although this point was not verified. Clearly the downfield shift in the ^{113}Cd NMR for the three sugar phosphate complexes, relative to $E_P(Cd)$, is associated with some aspect of the binding process rather than the subsequent PO_3^--transfer step.

[3] In the 6-dGlc-1-P system, the $E_P(Cd)$6-dGlc-1-P complex is in relatively slow exchange with the free sugar phosphate. There also is a minor additional complex, presumably a loose $E_P(Cd)$6-dGlc-1-P complex, that exhibits rapid or close to rapid exchange with free 6-dGlc-1-P.

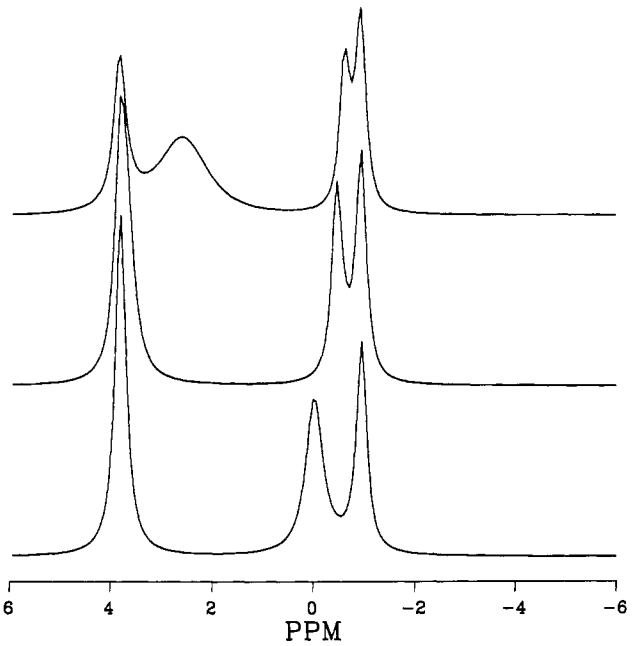

FIGURE 2: Line shape simulations of the ^{31}P NMR spectra in Figure 1. In these simulations the magnetic effect of ^{113}Cd was ignored, as were possible intensity differences arising from differences in T_1 values. The ratios of enzyme/Cd^{2+}/deoxysugar used in these simulations are the same as those given in the Figure 1 legend for b, c, and d of that figure.

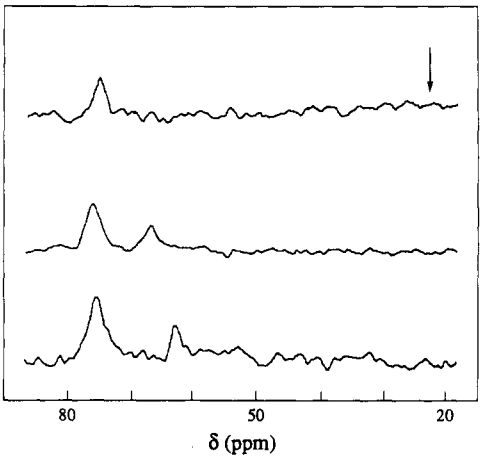

FIGURE 3: ^{113}Cd NMR spectroscopy of ternary substrate and substrate analog complexes of phosphoglucomutase. The binary Cd^{2+} complex of the phosphoenzyme was produced by addition of 1.0 equiv of $^{113}CdAc_2$ to the metal-free enzyme in 20 mM Tris-HCl, pH 7.5, which was present at a final concentration of 1.5 mM (upper plot) or 2.6 mM (lower two plots). After verifying the formation of the Cd^{2+} complex [^{113}Cd chemical shift of $E_P(Cd)$ = 22 ppm (arrow, upper plot) (Rhyu et al., 1984)] a small volume containing either 1 equiv of Glc-1-P (to produce $E_D(Cd)Glc\text{-}1,6\text{-}P_2$) (upper plot) or 5 equiv of 1-dGlc-6-P or 6-dGlc-1-P (middle or lower plots, respectively) was added. A total of 65 536 transients (upper plot) or 40 000 transients (middle and lower plots) were accumulated in the manner described previously (Rhyu et al., 1984). A line broadening of 40 Hz was applied prior to Fourier transformation. Chemical shifts refer to 0.1 M $Cd(ClO_4)_2$ in D_2O.

Electronic Spectrum of Substrate/Analog Complexes of the Co(II) and Ni(II) Enzymes. The electronic spectra of $E_P(Co)$ and $E_P(Ni)$ are shown in Figure 4, panels a and b, respectively (—), together with spectra of the respective complexes involving 1-dGlc-6-P (– – –), 6-dGlc-1-P, (---), and an equilibrium mixture of Glc-1-P + Glc-6-P (···). As in a number of related systems, the spectrum of Co^{2+} in the composite central complexes, ΣE(Co)Glc-P (not shown to avoid overlaps) can be mimicked by combining the spectra of

the two separate dGlc-P complexes according to the known ratio of 6-P:proximal and 6-P:distal complexes present [cf. the accompanying paper (Ray et al., 1993)]. The success of such a reconstruction indicates that in the dGlc-P complexes the absence of the hydroxyl group that normally is positioned to act as a PO_3^- acceptor does not substantially affect the ligand sphere of bound Co^{2+}. The same is not true for the Ni^{2+} enzyme (Figure 4b), where the spectral intensity of Ni^{2+} in the 1-dGlc-6-P complex is substantially greater than can be rationalized in terms of the corresponding fraction of 6-P:distal complexes in ΣE(Ni)Glc-P. In any case, the effective ligand field symmetry[4] in the various Glc-P/dGlc-P complexes resembles that of a number of pentacoordinate Co^{2+} complexes [$\epsilon \approx 200$ cm^{-2} M^{-1} in the visable range with substantial band splitting (Banchi et al., 1982; Bertini & Luchinat, 1984)][5] or of pentacoordinate Ni^{2+} complexes [enhanced prominance of both the 500-nm shoulder and substantially increased molar extinction of the near UV band relative to octahedral complexes (Ciampolini & Nardi, 1966, 1967; Dori & Grey, 1966; Sacconi et al., 1967; Rosenberg et al., 1975)]. In fact, the spectral differences among the various complexes could be caused by changes in length of a long apical bond in a pentacoordinate ligand sphere where the remaining ligands lie at the corners of a tetrahedron. However, such a mechanism fails to rationalize the effective ligand field symmetry of Ni^{2+} in E_P-(Ni) that appears to be octahedral-like (Ray & Multani, 1972). [Controls show that the following ions at a concentration of 0.1 M [which is much higher than the respective values of K_I, cf. Ray and Roscelli (1966)] also produce no significant changes in the electronic spectrum of Ep·Co: Br^-, I^-, SCN^-, $S_2O_3^{2-}$, SO_4^{2-}, and PO_4^{2-}; hence, it is unlikely that the above spectral changes are produced by the displacement of solvent/solute anions]. Whatever the origin, substrate-induced changes in the ligand sphere of the bound metal ion likely are produced indirectly, viz., without any group of the bound substrate/analog entering the ligand sphere of the metal ion (Y. Liu and W. J. Ray, Jr., preliminary model-building results).

Spatial Relationship of the Bound Metal Ion to the Enzymic Phosphate Group. Figure 5, top, is a stereographic view of selected residues in the active site region of the previously published model of the metal-free dephosphoenzyme (Dai et al., 1992), modified on the basis of the following considerations.

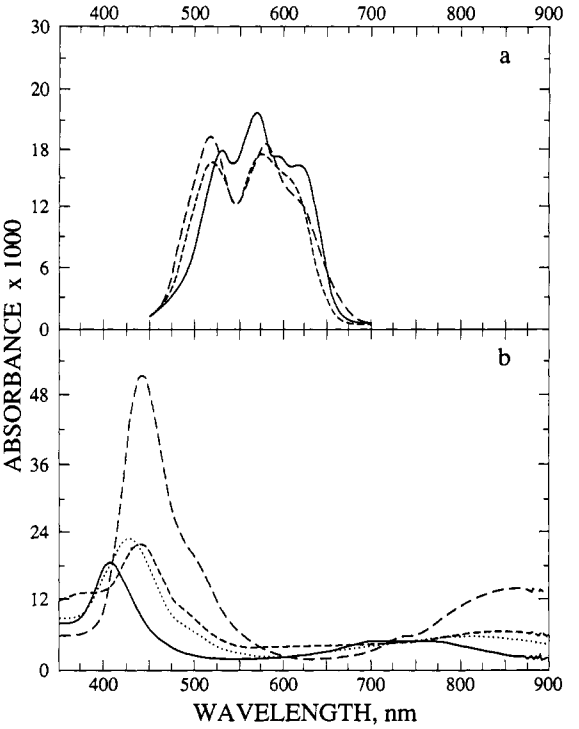

FIGURE 4: Effect of binding glucose phosphate and deoxy analogs thereof on the visible and near ultraviolet d–d transitions of Co^{2+} and Ni^{2+} bound to phosphoglucomutase. Spectra were obtained after mixing the contents of a sectored absorption cell with a light path of 0.427 cm per chamber; the general procedure was described previously (Ray et al., 1990). Prior to mixing, the absorption cell contained 0.800 mL of 0.29 mM metal-free enzyme (for Co^{2+} complexes) or 1.43 mM enzyme (for Ni^+ complexes) in one chamber and 0.800 mL of the sugar phosphate in the other, both in 20 mM Tris-HCl buffer, pH 7.5. After obtaining a baseline, the colored complex was generated first by replacing 0.100 mL of the sugar phosphate solution (that in some cases exhibited a faint yellow color) with 0.100 mL of the *same* solution that also contained sufficient $CoAc_2$ or $NiAc_2$ to provide 1.0 equiv of bivalent metal ion per equivalent of enzyme in the opposite chamber; the contents of both chambers then were mixed. The molar absorbances are larger than the measured absorbances (ordinate) by approximately 10^4 and 2×10^3-fold for the upper and lower plots, respectively. (a and b) Spectra of E_P(M) with the following additives: (—) none; (···) Glc-P; (– – –) 1-dGlc-6-P; (- - -) 6-dGlc-1-P.

When the structure factors for E_P(Cd) are used to define the X-ray term in X-PLOR (Brunger et al., 1989) and the above model is used for initial coordinates, energy minimization produces a refined model where by far the most prominent peaks in an $(F_o - F_c)$ electron density difference map (model phases) correspond with the positions expected for the enzymic phosphate group [attached to $Ser^{116}O\gamma$ (Ray et al., 1983)] and Cd^{2+} [which coordinates with the phosphate groups (Rhyu et al., 1984)], neither of which were included in the original model. Hence, these atoms were added, and further refinement was conducted. The postrefinement model (without further manual adjustment), together with the electron density in a $(2F_o - F_c)$ electron density map (model phases), is shown in Figure 5, top. Although the use of higher resolution data should improve the map, this figure is sufficient to suggest that a nonbridging oxygen (as opposed to a bridging oxygen; see Discussion) interacts directly with the bound metal ion in E_P(Cd). Similar results were obtained for the Ep·Mg complex, viz., the metal ion is centered in essentially the same position, in a somewhat smaller pocket due to reduced M···O distances, but is less well defined; the position of the phosphate is essentially unchanged at the current resolution. An examination of $(F_o - F_c)$ difference maps for the Ep·Cd complex, contoured at different density levels, plus various "omit maps"

[4] Coordination number and ligand field symmetry are closely related in metal ion complexes with a high symmetry but frequently are only distantly related in complexes with low symmetry, especially in complexes involving potentially bidentate ligands such as carboxylate. For example, in $Co[(CH_3)_2PO]_2(NO_3)_2$, Co^{2+} is surrounded by six ligands, but the effective symmetry of the ligand field more closely corresponds with a distorted tetrahedron where the bidentate nitrate group is considered as a single diffuse ligand centered at the position of its nitrogen (Cotton et al., 1963). The effective symmetry of the pentacoordinate Co^{2+} complex of carboxypeptides (Hardman et al., 1984) can be viewed similarly (Bertini & Luchinot, 1984). Alternatively, the effective symmetry of the five ligands that form a square pyramid can be considered in terms of axially-distorted octahedral-like coordination. Hence, to avoid overinterpreting our data, we sometimes refer to "effective ligand field symmetry", as opposed to coordination number. In order that coordination number not be a function of bond angles, a possibly bidentate carboxylate group, for example, is counted as a single ligand regardless of how close it might come to true bidentate coordination.

[5] The effective ligand field of Co^{2+} in E_P(Co) has been interpreted in terms of tetrahedral-like symmetry (Ray & Multani, 1972). However, subsequent studies of model Co^{2+} complexes [cf. Banci et al. (1982) and Bertini & Luchinat (1984)] show that tetrahedral/pentahedral symmetries can be difficult to distinguish on the basis of electronic spectra. Hence, although the effective ligand field in E_P(Co) seems to be pentahedral-like, the spectrum of E_P(Co) more closely resembles that of $CoAc_4^{2-}$ than that of any known pentacoordinate Co^{2+} complex (W.J.R., unpublished results).

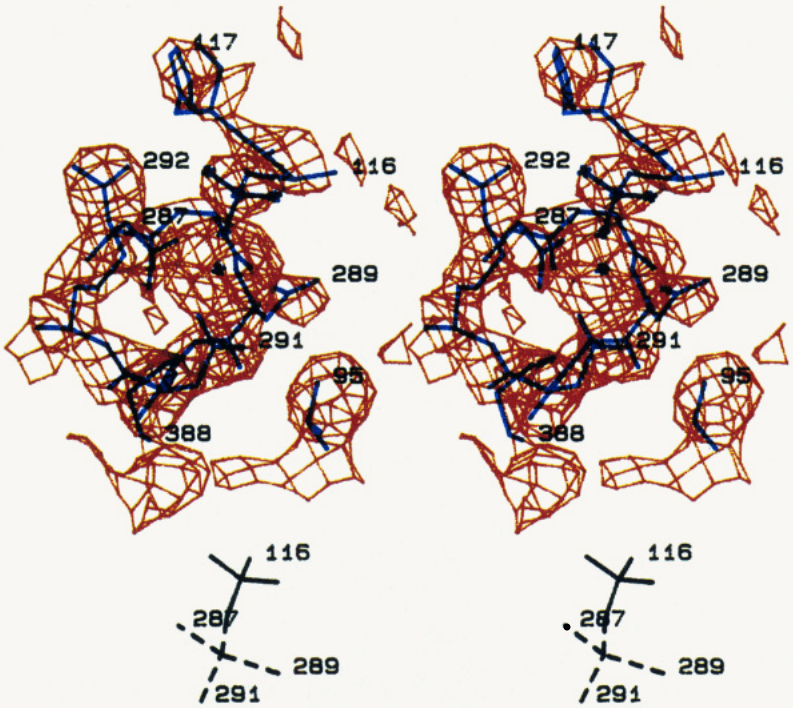

FIGURE 5: Stereographic views of the active site of phosphoglucomutase. (Top) The previously published model (Dai et al., 1992) to which has been added a PO_3 group (attached at $Ser^{116}O\gamma$) and a metal ion, Cd^{2+}; added atoms are indicated by +. The electron density in a map calculated as $(2F_o - F_c)$ with model phases also is shown. The following atoms are identified by residue number: $Thr^{95}O\gamma$, Ser-$P^{116}O\gamma$, $His^{117}N\delta$, $Asp^{287}O\delta$, $Asp^{289}O\delta$, $Asp^{291}O\delta$, $Arg^{292}N\epsilon$, and $Lys^{388}N\zeta$. (Bottom) The positions of Cd^{2+}, the four atoms of the protein that serve as primary ligands, and the remaining atoms of the enzymic phosphate group are shown. ($Ser^{116}O\gamma$ is the phosphate oxygen that is labeled; the other three are Asp Oδ oxygens.) The solid lines interconnect the atoms of the phosphate group; the dashed lines indicate coordinate interactions involving the metal ion.

suggest that the M···OP interaction involves a single nonbridging oxygen, as also is suggested by the narrowing of the electron density between Cd^{2+} and the phosphate oxygens (Figure 5, top). However, at present this conclusion must be considered as tentative (see Discussion). Although with the current data the (Mg^{2+}·$^{2-}O_3P^-$) interaction thus cannot be specified in terms of one or two ligands, a comparison of electron density maps indicates that this interaction is closely similar to that involving Cd^{2+}.

Only four metal–protein ligands can be identified in Figure 5, top: the Oδ of aspartates 287, 289, and 291 in the metal binding loop (Dai et al., 1992) and the nonbridging phosphate oxygen. (The "other Oδ" of Asp^{287} is 3.4 Å from the Cd^{2+} and thus coordinates exceedingly weakly with the metal ion if at all.) However, there is room for an axial water molecule if Asp^{287} is considered as the other axial ligand (Figure 5, bottom), which shows the approximate tetrahedral geometry of the metal ion site: (dashed lines) average Cd···O bond distance, 2.05 ± 0.15 Å, standard deviation from tetrahedral angles was ±7° without manual adjustment of the computer-generated model. A more regular tetrahedral array can be constructed easily by minor manual adjustments of atoms within the density. Although there is no density in this map indicating that a water molecule acts as a fifth ligand, in the Mn^{2+} enzyme water appears to have access to the primary coordination sphere of the metal ion (Ray & Mildvan, 1970), and the temperature dependence of the electronic spectrum of Co^{2+} in E_P(Co) (Ray & Multani, 1972) is most easily rationalized in terms of the addition of a water molecule to the ligand sphere of bound Co^{2+}. It is unlikely that any of the three aspartic acid side chains in the metal binding loop acts as a bidentate ligand, since in each case there is a potential for hydrogen bonding of the nonligaled carboxylate oxygen to other protein groups.

DISCUSSION

Ideally, if an acceptor oxygen is positioned in the manner illustrated in Scheme Ia, the only major geometrical requirement for PO_3^- transfer is the horizontal displacement of phosphorus (dashed arrow) by 1–1.5 Å, depending on the proximity of the acceptor oxygen [cf. Jones et al. (1991)]. Many PO_3^- transferases likely utilize this process (Herschlag & Jencks, 1990), which is that expected for a dissociative reaction via the "exploded" transition state that characterizes all model PO_3^- transfer reactions of phosphate ester *dianions* (Allen & Haake, 1980; Bourne & Williams, 1984; Skoog & Jencks, 1984; Jencks, 1985; Herschlag & Jencks, 1987, 1989a,b; Williams, 1987). But there are additional constraints on the phosphoglucomutase reaction. Thus, all components of the catalytic apparatus for PO_3^- transfer, other than the acceptor, are present in the enzyme. But for optimal metabolic efficiency, the enzyme must not transfer its PO_3^- group to any passing acceptor, including water, and the substrate/water discrimination factor is some 3×10^{10}-fold (Ray et al., 1976). (As can be deduced from Figure 5, top, the accessibility of water to the phosphate group in the region opposite $Ser^{116}O\gamma$ is not a factor in this ratio.) Another requirement is that the metabolically important process not end with the first transfer step but include an isomerization of the intermediate bisphosphate complex in which the two phosphate groups of the bisphosphate are exchanged intramolecularly, i.e., without complete dissociation of the bisphosphate [Ray & Roscelli, 1964; see also the accompanying paper, Ray et al. (1993)]. This isomerization requires a significant disruption of binding interactions since these two phosphate sites are approximately 10 Å apart (Ray & Mildvan, 1973). In addition, the metabolic role of the enzyme requires that it operate with a high degree of efficiency in *both* the forward and reverse directions. The involvement of the bivalent metal ion activator may provide

Scheme I: Comparison of Relative Positions of Atoms, Including a Metal Ion Coordinating to a Nonbridging Oxygen, before and after a PO_3^- Transfer Involving Dissociative and Associative Processes[a]

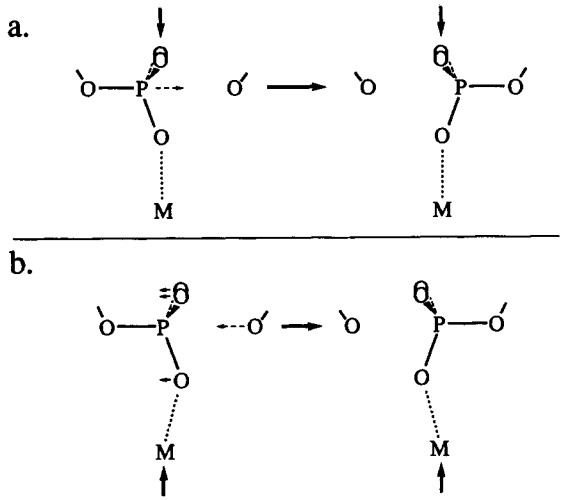

[a] Relative bond lengths for P–O and O···M were taken as 1.5 and 2.0 Å, respectively, and O–P–O bond angles are represented as being tetrahedral; the P–O···M bond angle is arbitrary. The heavy vertical arrows on the reactants side and products side of the reaction indicate the atoms that are displaced least by the reaction; the small dashed arrows indicate the movement of the atoms that undergo the greatest displacement. (a) An idealized representation of a dissociative process where the primary positional displacement, or impetus for reaction, involves the movement of phosphorus from left to right; a metal ion coordinating to a nonbridging oxygen is positioned so that the M···O–P interaction is the same in the reactants and products, assuming that the positions of the nonbridging oxygen as well as the incoming oxygen are unchanged. (b) A related representation of an associative process where the primary impetus involves movement of the incoming oxygen from right to left; a metal ion coordinated as in panel a is positioned so that the M···O–P bond angle is the same in reactants and products.

a further constraint. Thus, in the "resting" $E_P(M)$ complex, there is a direct (M^{2+}·$^{2-}O_3P^-$) interaction (Rhyu et al., 1984) that, on the basis of the present results, involves a nonbridging oxygen (Figure 5, top). But, in the dephosphoenzyme, what origianlly was the bridging oxygen in $E_P(M)$, $Ser^{116}O\gamma$, takes the place of the departed nonbridging oxygen in the coordination sphere of the metal ion (Dai et al., 1992), ostensibly to "cap" the metal binding pocket and prevent the rapid dissociation of bound Mg^{2+} [$\tau_{1/2}$ for dissociation of Mg^{2+} from $E_P(Mg)$ and $E_D(Mg)$ is ≈25 and 10 s, respectively (Ray & Roscelli, 1966)].

All of the above constraints may influence how the enzyme conducts the PO_3^- transfer process, but some become less of a problem if the active site of the enzyme exhibits a suitable degree of flexibility. And a significant flexibility is not surprising since the groups acting, respectively, as the PO_3^- donor/acceptor, the metal-binding loop, the sugar-binding pocket, and the distal phosphate binding site reside primarily in four distinct (but contiguous) domains (Dai et al., 1992). In order to determine whether various structural changes, some of which were described earlier (Rhyu et al., 1985), are related to the PO_3^- transfer step per se or to other aspects of the phosphoglucomutase reaction, two deoxyglucose phosphate inhibitors and three different metal ion activators were used as active site probes.

The present results, together with results from previous studies, show that some of the structural changes at the metal binding site occur during Glc-P/dGlc-P binding: the downfield shift in the ^{113}Cd NMR of E_P·Cd (Rhyu et al., 1985a; Results), the change in the electronic spectrum of E_P·Co and E_P·Ni (Figure 3), and changes in the EPR spectrum of E_P·Mn (Reed & Ray, 1971). Unfortunately, we cannot be certain that the starting point is the same in all cases, viz., that the ligand sphere of the metal ion is identical in each E_P·M complex, both because of the possibility that the process of crystallization alters the coordination sphere of the metal ion (cf. Lin et al., 1991) and because of the relatively low resolution of our diffraction data: about 2.7 Å (and thus the uncertain involvement of water molecules, plus the possibility that one or more ligands coordinates in a bidentate manner). Thus, the ligand sphere of Cd^{2+} in $E_P(Cd)$ contains four ligands (Figure 5): three carboxylates and the nonbridging oxygen of a phosphate ester dianion. Mg^{2+} in $E_P(Mg)$ is bound similarly (Results), as is likely the case in $E_P(Co)$, since Co^{2+} exhibits a substantially greater propensity toward such coordination (Cotton & Wilkinson, 1980). But the Ni^{2+} enzyme appears to be substantially different [cf. Ray and Multani (1972)],[5] possibly because, relative to Co^{2+}, it exhibits an aversion toward a tetracoordinate environment (Cotton & Wilkinson, 1980).

In $E_P(Cd)$ each ligand appears to be monodentate (see Results), and probable hydrogen-bonding patterns (not shown) support this suggestion. Whether or not in other complexes a carboxylate ligand is more nearly bidentate, a tetracoordinate ligand sphere[4] seems more suitable than a more crowded hexacoordinate sphere for allowing changes in the P–O···M interaction within the ternary complexes *during* the PO_3^- transfer step (see below). In fact, we attach a substantial significance to Nature's "decision" to use a tetracoordinate binding site for Mg^{2+}, since the consequence of using such an array, which is more compatible with Zn^{2+} binding, is that more than half of the phosphoglucomutase in muscle cells is present as the relatively inactive Zn^{2+} form of the enzyme: activity ~0.001 of the Mg^{2+} enzyme (Peck & Ray, 1970; Magneson et al., 1986).

The origin of the substrate/substrate analog-induced *changes* in metal ion coordination likely is the same in $E_P(Cd)$ and $E_P(Co)$, and the observed changes probably reflect what occurs in $E_P(Mg)$ also. These changes are in the direction expected for (a) a decreased number of ligands for Cd^{2+} (Armitage & Otvos, 1982) or a geometrically altered ligand sphere and (b) an increased number of ligands for Co^{2+} (Bianchi et al., 1982; Bertini & Luchinat, 1984) or a geometrically altered ligand sphere. Hence, in both cases we opt for a rationale where a geometrically altered ligand sphere accounts for the induced changes. A more irregular ligand sphere for bound Mn^{2+} also is in accord with the substrate-induced changes in the EPR signal of $E_P(Mn)$ (Reed & Ray, 1971). Only in the case of Ni^{2+} is it difficult to explain the induced spectral changes with such a model; at present we have no rationale for the apparently aberrant properties of $E_P(Ni)$. From an energetic standpoint, there is no indication that the substrate-induced change at the metal-binding site is substantially energy requiring, since the equilibrium binding of three different metal ions, Mg^{2+}, Cd^{2+}, and Zn^{2+}, is relatively unaffected by the presence of bound substrate (Ray et al., 1966; W.J.R. unpublished results). Hence, the observed change may reflect what is required to *allow* catalysis to proceed efficiently, rather than serving to drive the PO_3^- transfer proces; viz., the observed changes probably do not require a substantial fraction of the intrinsic binding energy of the substrate.

Other changes occur subsequent to the binding step. One such change involves the J_{CdP} coupling that characterizes the direct (Cd^{2+}·$^{2-}O_3P^-$) interaction in $E_P(Cd)$. That coupling,

which is retained in the E_P(Cd)dGlc-P inhibitor complexes (cf. Figure 1), is either absent or substantially reduced in E_D(Cd)Glc-P_2, and the change in this coupling thus is associated with either the transfer step that converts E_P(Cd)-Glc-P into the bisphosphate complex or a subsequent step that prepares the E_D(Cd)Glc-P_2 complex for the rearrangement of the bisphosphate moiety. In fact, since the size of J_{CdP} in E_P(Cd) and E_P(Cd)dGlc-P is similar, the (Cd^{2+},$^{2-}O_3P^-$) interaction in the normal substrate complex may well be similar in the binary and ternary E_P·Cd complexes.

Unfortunately, neither the point during the reaction when the above J_{CdP} coupling is lost nor the structural basis for the loss can be defined with the present data. It is possible that the loss is caused by the departure of the nonbridging phosphate oxygen from the coordination sphere of Cd^{2+} to facilitate either the development of a negative charge on the departing $Ser^{116}O\gamma$ (during PO_3^- transfer to Glc-P) or the subsequent internal rearrangement of the bisphosphate within the E_D(Cd)Glc-P_2 complex thus formed. If the loss in *J* coupling occurs *during* the transfer process so that the P–O···M interaction associated with E_P(Cd) is replaced by the C–O···M interaction involving $Ser^{116}O\gamma$ that characterizes *free* E_D(Cd) (Dai et al., 1991), the structural changes that accompany the transfer step would be substantial, indeed. If this loss occurs just *prior to* the partial dissociation that accompanies the rearrangement step [cf. the accompanying paper (Ray et al., 1993)] or only *after* complete dissociation of the bisphosphate, the size of the structural change might well be just as large, but it would be less striking. Since these possibilities cannot be distinguished, as of now, we concentrate instead on changes that occur between E_P(M) plus bound Glc-1-P and the transition state for the first PO_3^- transfer step.

As noted above, the interaction of a metal ion with a nonbridging oxygen in an enzyme–substrate complex may place restrictions on how the PO_3^- transfer occurs. In Scheme Ia, where for facile presentation the –O–P–O···M constellation is taken as coplanar, in order that the only major displacement during PO_3^- transfer involve the phosphorus nucleus (dashed arrow) and that the metal ion interact with the P–O groups of reactants and products in the same way, the metal ion must lie close to the plane of the nonbridging oxygens. If not, a more extensive movement of atoms is required, as in Scheme Ib, where it is primarily the oxygens that change their positions (dashed arrows) while the phosphorus remains more or less stationary, or else there will be a change in what we presume is a preferred P–O···M bond angle (not shown).

Clearly, in Figure 5, bottom, the Cd^{2+} is not in the plane of the nonbridging oxygens. And although the metal ion is closer to that plane in E_P(Mg), in binary complexes the (M^{2+},$^{2-}O_3P^-$) interaction still is similar to that depicted in Scheme Ib. Hence, we consider two different scenarios. One is that substrate binding aligns the (M^{2+},$^{2-}O_3P^-$) grouping so that a process related to that illustrated in Scheme Ia transpires, viz., PO_3^- transfer occurs via an "exploded" transition state. In such a case, failure to obtain this alignment in the absence of the substrate could provide a partial rationale for the substrate/water specificity ratio noted above. On the other hand, if the above alignment is not realized in the presence of bound substrate, the likely scenario would be closer to that in Scheme Ib. In such a case, the incoming oxygen might play a more important role in the reaction, as it does in the initial phase of phosphate diester hydrolysis [cf. Benkovik and Schray (1978), Knowles (1980), and Hengge and Cleland (1991)]. We favor the latter possibility in the phosphoglucomutase reaction, partly because J_{CdP} does not seem to change on the binding of the dGlc-P inhibitors, partly because of the manner in which the vanadate group in the "transition-state analog" complex, E_D(Mg)V-6-Glc-1-P, is polarized (H. Deng, W. J. Ray, Jr., J. W. Burgner, II, and R. Callender, manuscript in preparation), and partly because the above study suggests that the primary involvement of the metal ion is with the nonbridging oxygen during approach to the transition state. Although it is not possible in the phosphoglucomutase reaction, if two metal ions were involved in the PO_3^- transfer, as in the alkaline phosphatase reaction (Kim & Wyckoff, 1991), a nonbridging oxygen could shuttle between two different metal ions to accommodate changes in bond distances/angles during the forward and reverse phases of the transfer process.

But as Jones et al. (1990) point out, it is not considerations such as those above, but the bond order of entering and leaving oxygens that provides a rigorous distinction between associative and dissociative PO_3^- transfer. On the other hand, although such an assessment can be made in some enzymic systems [see also Hall and Williams (1985)], in many others evaluating bond order in the transition state is difficult or impossible. In such cases, evaluating which atoms move in proceeding from reactants to products, and by how much (actually evaluating where the impetus for the reaction lies), may be informative. Thus, the change in charge density associated with groups surrounding phosphorus en route to the transition state should be related to changes in bond order. Moreover, atomic movement and bond polarization likely are more closely linked than, for example, in sn_1 and sn_2 reactions at carbon when the attached groups are saturated. Thus, in a dissociative PO_3^- transfer, as the bridging P–O bond lengthens, nonbridging P–O bonds become shorter [so as to conserve the overall bond order of phosphorus (Cleland, 1990)]. This produces an inverse ^{18}O secondary kinetic isotope effect (Jones et al., 1991). By contrast, if an oxygen is to mount a successful attack on the electropositive phosphorus of a phosphate ester *dianion*, the negative electrostatic charge associated with the nonbridging oxygens must be substantially reduced, to a point at least comparable to that in a phosphate ester monoanion (Knowles, 1980), so that nonbridging P–O bonds are lengthened in the transition state; this would produce the opposite type of isotopic behavior. Thus, in a predominantly dissociative process (Scheme Ia) the electrostatic charge initially associated with the nonbridging oxygens must "flow" toward the leaving group via the phosphorus; in a predominately associative process, the flow of the same charge must be away from the phosphorus toward the negative end of the P–O dipole, thereby providing a facile mechanism for increasing interactions between these oxygens and catalyst in the transition state (Knowles, 1980). Although an associative-type reaction involving a phosphate ester *dianion* in aqueous solution is without precedence (Herschlag & Jencks, 1990) and cannot be accomplished via whatever polarization can be achieved by metal ion binding in such solutions (Herschlag & Jencks, 1987), the existence of a tetracoordinate Mg^{2+} complex in contact with water, as in E_P(Mg), also is without precedence [cf. Adams et al. (1963) and Shannon and Berzius (1979)]. Hence, in view of the potential that a tetracoordinate metal binding site provides for the motion of a nonbridging oxygen coordinated with that metal ion and the consequences of that coordination (see below), we consider a predominately associative process as a distinct possibility in the phosphoglucomutase reaction.

In fact, the transition state binding paradigm of enzyme catalysis requires that there be a large increase in the strength of the (M^{2+},$^{2-}O_3P^-$) interaction en route to the transition state

of the phosphoglucomutase reaction, since the transfer process is exceedingly slow when Li^+ is substituted for Mg^{2+} (Ray et al., 1989) or when the metal ion removed completely (W.J.R., unpublished results). Such an increase more closely accords with a transition state where the effective electrostatic charge on nonbridging oxygens becomes more negative at the expense of the central phosphorus and the incoming oxygen, so that the charge density associated with that oxygen acquires much greater importance than in the dissociative process [cf. Williams (1989)]. But this implies that the M···O–P interaction in the transition state involves a nonbridging oxygen and not the bridging oxygen. Thus, one way to provide support for an associative-type process in the present system would be to show that the metal ion does not coordinate with $Ser^{116}O\gamma$ in the transition state when the enzyme is acting as a PO_3^- donor. Although the use of a transition-state analog inhibitor complex (Ray & Puvathingal, 1984) may help to decide this point, we note that structural considerations make it unlikely that the metal ion interacts with the bridging oxygen (to glucose) in the reverse process where Glc-P_2 is the PO_3^- donor (see Figure 5) since the substrate must bind in front of the and above the enzymic phosphate group. Restricting the metal ion to a possible interaction with only one of the two bridging oxygens involved in the overall process greatly reduces the attractiveness of a dissociative reaction. Although metal ion binding to $Ser^{116}O\gamma$ would facilitate transfer of the enzymic PO_3^- group to Glc-P, the same interaction would be relatively ineffective in the reverse reaction which, according to microscopic reversibility, must be dissociative if the forward process is. But in model reactions, the rate of a dissociative PO_3^- transfer is quite insensitive to the basicity of the *incoming* oxygen. Hence, the reduced pK_a of $Ser^{116}O\gamma$ that would be produced by metal ion coordination would be ineffective in facilitating a dissociative PO_3^- transfer where that oxygen is the acceptor. Put a different way, the dissymmetric involvement of a metal ion with one of two donor/acceptor oxygens in any PO_3^- transfer process is tantamount to a change in rate that will be reflected to a substantial extent by a change in equilibrium constant. Since substituting Li^+ for Mg^{2+} at the metal-binding site changes the rate of PO_3^- transfer by some 2.5×10^{-9}-fold but scarcely changes the equilibrium constant (Ray et al., 1989), we favor a more symmetrical involvement of the metal ion with a bridging oxygen, as in the resting enzyme (Figure 5), and thus a transfer process that for this enzyme is more nearly associative than dissociative.

REFERENCES

Adams, D. M., Chatt, J., Davidson, J. M., & Gerrall, J. (1963) *J. Chem. Soc.*, 2189–2199.

Allen, G. W., & Haake, P. (1980) *Bioorg. Chem. 9*, 325–341.

Armitage, I. M., & Otvos, J. D. (1982) *Biol. Magn. Reson. 4*, 79–144.

Banci, L., Bencini, A., Benelli, C., Gatteschi, D., & Zanchini, C. (1982) *Struct. Bonding (Berlin) 52*, 37–86.

Benkovik, S. J., & Schray, K. J. (1978) *Enzymes (3rd Ed.) 8*, 201–238.

Bertini, I., & Luchinat, C. (1984) in *Advances in Inorganic Biochemistry* (Eichhorn, G. L., & Marzilli, Eds.) Vol. 6, Elsevier, New York.

Bourne, N., & Williams, A. (1984) *J. Org. Chem. 49*, 1200–1204.

Brunger, A. T., Krukowski, A., & Erickson, J. W. (1989) *J. Crystallogr. A46*, 585–593.

Ciampolini, M., & Nardi, N. (1966) *Inorg. Chem. 5*, 41–44.

Ciampolini, M., & Nardi, N. (1967) *Inorg. Chem. 6*, 445–449.

Cleland, W. W. (1990) *FASEB J. 4*, 2899–2905.

Cotton, F. A., & Wilkinson, G. (1980) *Advanced Inorganic Chemistry*, 4th ed., pp 686–687, Wiley, New York.

Cotton, F. A., Goodgame, D. M. L., & Soderberg, R. H. (1963) *Inorg. Chem. 2*, 1162–1165.

Dai, J.-B., Liu, Y., Ray, W. J., Jr., & Konno, M. (1992) *J. Biol. Chem. 267*, 6322–6337.

Dori, Z., & Gray, H. B. (1966) *J. Am. Chem. Soc. 88*, 1394–1398.

Hall, A. D., & Williams, A. (1985) *J. Chem. Soc., Chem. Commun.*, 1680–1681.

Hammond, G. S. (1955) *J. Am. Chem. Soc. 77*, 334–338.

Hardman, K. D., & Lipscomb, W. N. (1984) *J. Am. Chem. Soc. 106*, 463–464.

Hengge, A. C., & Cleland, W. W. (1991) *J. Am. Chem. Soc. 113*, 5835–5841.

Herschlag, D., & Jencks, W. P. (1987) *J. Am. Chem. Soc. 109*, 4665–4674.

Herschlag, D., & Jencks, W. P. (1989a) *J. Am. Chem. Soc. 111*, 7579–7586.

Herschlag, D., & Jencks, W. P. (1989b) *J. Am. Chem. Soc. 111*, 7587–7596.

Herschlag, D., & Jencks, W. P. (1990) *Biochemistry 29*, 5172–5179.

Jencks, W. P. (1985) *Chem. Rev. 85*, 511–527.

Jones, J. P., Weiss, P. M., & Cleland, W. W. (1991) *Biochemistry 30*, 3634–3639.

Jones, T. A. (1978) *J. Appl. Crystallogr. 11*, 268–274.

Kim, E. E., & Wyckoff, H. (1991) *J. Mol. Biol. 218*, 449–464.

Knowles, J. R. (1980) *Annu. Rev. Biochem. 49*, 877–919.

Lin, S.-L., Stern, E. A., Kalb, A. J., & Xhang, Y. (1991) *Biochemistry 30*, 2323–2332.

Ma, C., & Ray, W. J., Jr. (1980) *Biochemistry 19*, 751–795.

Magneson, G. R., Puvathingal, J. M., & Ray, W. J., Jr. (1987) *J. Biol. Chem. 262*, 11140–11148.

Peck, E. J., Jr., & Ray, W. J., Jr. (1970) *J. Biol. Chem. 246*, 1160–1167.

Post, C. B., Ray, W. J., Jr., & Gorenstein, D. G. (1989) *Biochemistry 28*, 548–558.

Ray, W. J., Jr. (1969) *J. Biol. Chem. 244*, 3740–3747.

Ray, W. J., Jr., & Roscelli, G. A. (1964) *J. Biol. Chem. 239*, 1228–1236.

Ray, W. J., Jr., & Roscelli, G. A. (1966) *J. Biol. Chem. 241*, 1012–1014.

Ray, W. J., Jr., & Mildvan, A. S. (1970) *Biochemistry 9*, 3886–3894.

Ray, W. J., Jr., & Multani, J. S. (1972) *Biochemistry 11*, 2805–2812.

Ray, W. J., Jr., & Mildvan, A. S. (1973) *Biochemistry 12*, 3733–3743.

Ray, W. J., Jr., & Long, J. W. (1976a) *Biochemistry 15*, 3993–4006.

Ray, W. J., Jr., & Long, J. W. (1976b) *Biochemistry 15*, 4018–4025.

Ray, W. J., Jr., & Puvathingal, J. M. (1984) *J. Appl. Crystallogr. 17*, 372.

Ray, W. J., Jr., Roscelli, G. A., & Kirkpatrick, D. S. (1966) *J. Biol. Chem. 241*, 2603–2610.

Ray, W. J., Jr., Goodin, D. S., & Ng, L. (1972) *Biochemistry 11*, 2800–2804.

Ray, W. J., Jr., Long, J. W., & Owens, J. D. (1976) *Biochemistry 15*, 4006–4017.

Ray, W. J., Jr., Hermodson, M. A., Puvathingal, J. M., & Mahoney, W. C. (1983) *J. Biol. Chem. 258*, 9166–9174.

Ray, W. J., Jr., Post, C. B., & Puvathingal, J. M. (1989) *Biochemistry 28*, 559–569.

Ray, W. J., Jr., Burgner, J. W., II, & Post, C. B. (1990) *Biochemistry 29*, 2770–2778.

Ray, W. J., Jr., Puvathingal, J. M., & Liu, Y. (1991) *Biochemistry 30*, 6875–6885.

Ray, W. J., Jr., Post, C. B., & Puvathingal, J. M. (1993) *Biochemistry* (preceding paper in this issue).

Reed, G. H., & Ray, W. J., Jr. (1971) *Biochemistry 10*, 3190–3197.
Rhyu, G. I., Ray, W. J., Jr., & Markley, J. L. (1984) *Biochemistry 23*, 252–260.
Rhyu, G. I., Ray, W. J., Jr., & Markley, J. L. (1985a) *Biochemistry 24*, 2536–2541.
Rhyu, G. I., Ray, W. J., Jr., & Markley, J. L. (1985b) *Biochemistry 24*, 4746–4753.
Rosenberg, R. C., Root, C. A., & Gray, H. B. (1975) *J. Am. Chem. Soc. 97*, 21–26.
Sacconi, L., Bertini, I., & Morassi, R. (1967) *Inorg. Chem. 6*, 1548–1553.
Shannon, R. D., & Berzius, T. (1979) *Mater. Res. Bull. 14*, 361–367.
Skoog, M. T., & Jencks, W. P. (1984) *J. Am. Chem. Soc. 106*, 7597–7606.
Weiss, P. M., & Cleland, W. W. (1989) *J. Am. Chem. Soc. 111*, 1928–1929.
Williams, A. (1987) in *Enzyme Mechanisms* (Page, M. I., & Williams, A., Eds.) pp 97–122, Royal Society of Chemistry, London.
Williams, A. (1989) *Acc. Chem. Res. 22*, 387–392.

APPENDIX: NMR LINE SHAPE ANALYSIS AND ENZYME BINDING

Multisite Line Shape Analysis. NMR spectral line shapes can be used to study binding in protein–ligand systems (Crothers et al., 1974; Rao, 1989) when the kinetic rates are near the time scale of the chemical shift difference of the resonance frequencies corresponding to the different kinetic states. The analysis of line widths and peak position can distinguish kinetic schemes differing in binding order and provides estimates for the exchange rates (McConnell, 1953). (Since spin coupling effects are not a factor in ^{31}P exchange NMR studies, spin coupling is not addressed here.) For many of the reported NMR exchange studies on small molecules, the exchange process is due to internal conformational changes. In an enzymic system, additional processes which lead to exchange include bimolecular ligand binding and chemical reaction. To our knowledge, only Vasavada, Kaplan, and Rao (Vasavada et al., 1980; Rao, 1989) have previously reported the use of line shape analysis on enzymic systems.

In the case of phosphoglucomutase, the systems studied have two magnetic nuclei undergoing exchange due to binding—the ^{31}P nucleus of the ligand and that of the phosphoenzyme. Hence, additional constraints are involved; the spectral characteristics of two sets of exchange sites must be consistent with the same association/dissociation rate constants.

We describe an approach with general applicability for the line shape analysis of intermediate to fast exchange processes in enzymic systems. The approach involves a matrix form of the simultaneous Bloch equations for the transverse magnetization including chemical exchange to account for exchange among all possible sites in a multisite system.

Analogous approaches have been reported for the analysis of saturation transfer NMR pertaining to exchange processes which are slow on the chemical shift time scale (Perrin & Gipe, 1984; Grassi et al., 1986; Johnston et al., 1986; Mendz et al., 1986; Post et al., 1989). In saturation transfer studies, the change in peak intensities, or longitudinal z-magnetization, in response to the selective irradiation of a peak is measured. That is, a time-dependent intensity change due to a perturbation from equilibrium is analyzed. In contrast, this work concerns systems undergoing more rapid exchange for which the changes in line widths and peak position in the equilibrium spectrum as a function of ligand concentration can be used to estimate rate constants. These exchange studies are concerned with transverse magnetization whose description requires complex quantities, as opposed to longitudinal magnetization and real quantities.

The matrix form for the exchange system arises from the Bloch equations (Sandström, 1982) for the transverse components of magnetization in the rotating frame. The time dependences of the transverse components u and v from spin A after the application of a radio-frequency pulse B_1 are

$$\frac{du}{dt} = 2\pi v(\nu_A - \nu) - \frac{u}{T_2^A} \tag{1}$$

$$\frac{dv}{dt} = -2\pi u(\nu_A - \nu) - \frac{v}{T_2^A} + \gamma B_1 M_0^A \tag{2}$$

T_2^A is the transverse relaxation time, ν_A is the resonance frequency of spin A, γ is the gyromagnetic ratio, and M_0^A is the equilibrium z-magnetization.

The magnetization in the x–y plane is $M_A = u + iv$ and has the following time dependence:

$$\frac{dM_A}{dt} = -\left[\frac{1}{T_2^A} + i2\pi(\nu_A - \nu)\right] M_A + i\gamma B_1 M_0^A \tag{3}$$

The final term in eq 3 is a constant factor dependent on experimental conditions which reflects the total equilibrium magnetization intensity of spin A. Equation 3 simplifies to

$$\frac{dM_A}{dt} = -\alpha_A M_A + iC_A \tag{4}$$

$$\alpha_A \equiv \frac{1}{T_2^A} + i2\pi(\nu_A - \nu) \tag{5}$$

$$C_A \equiv \gamma B_1 M_0^A \tag{6}$$

In the case of chemical exchange, eq 4 must be modified to account for the interconversion of the nucleus among magnetically inequivalent sites. The kinetic rate constants are defined by

$$\mathrm{A} \underset{k_{BA}}{\overset{k_{AB}}{\rightleftarrows}} \mathrm{B} \tag{7}$$

The relative populations may be expressed as

$$\frac{f_A}{f_B} = \frac{k_{BA}}{k_{AB}} \tag{8}$$

and the fractional populations over all possible sites available to that nucleus satisfy the condition

$$\sum_i f_i = 1 \tag{9}$$

The effects of exchange among N sites are accounted for by modifying eq 4. The transverse magnetization corresponding to site i in exchange with all other sites j is

$$\frac{dM_i}{dt} = -\alpha_i M_i + if_i C_i - \sum_{j \neq i}^{N} k_{ij} M_i + \sum_{j \neq i}^{N} k_{ji} M_j \tag{10}$$

At equilibrium, $dM_i/dt = 0$ for all spins, and the set of N simultaneous equations in matrix form becomes

$$\mathbf{K} = \mathbf{\Omega G} \tag{11}$$

where the elements of the complex vectors **K** and **G** and the

$N \times N$ complex matrix Ω are

$$K_i = -if_iC_i \tag{12}$$

$$G_i = M_i \tag{13}$$

$$\Omega_{ii} = -(\alpha_i + \sum_{j \neq i}^{N} k_{ij}) \tag{14}$$

$$\Omega_{ij} = k_{ji}$$

The complex spectrum is found by determining G as a function of frequency ν, with the absorptive mode being the sum of the N imaginary elements of G. Equation 11 was solved by using the subroutine LEQT1C in the IMSL library.

Application to Enzymic Exchange Systems. To illustrate the application of eq 11 to exchange systems involving enzymes and enzyme–ligand complexes, the calculation of the equilibrium spectrum for the process shown in Scheme I is described.

The rate constants in the elements of Ω, eq 14, are defined in terms of the kinetic rate constants

$$k_{14} = k_1[S_p] \quad k_{35} = k_1[E_p] \quad k_{53} = k_{-1} \quad k_{73} = k_{-2}$$

$$k_{12} = k_3 \quad k_{37} = k_2[E_p] \quad k_{57} = k_4 \quad k_{75} = k_{-4}$$

$$k_{21} = k_{-3} \quad k_{41} = k_{-1} \quad k_{62} = k_{-2}$$

$$k_{26} = k_2[S_p] \quad k_{46} = k_4 \quad k_{64} = k_{-4}$$

All other rate constants in Ω correspond to nonexistent exchange processes and are set equal to 0.0.

A spectrum is calculated by using values for $[E_p]$ and $[S_p]$ determined from the known, total enzyme and ligand concentrations and equilibrium constants estimated from the integrated NMR intensities. The individual values for T_2^i and the intrinsic resonance frequencies ν_i are apparent from the NMR spectrum at limiting concentrations or initial values are estimated. Initial estimates of the kinetic rates in Scheme I are made, and the calculated and measured spectra at different total concentrations are compared. The kinetic rates, and in some cases T_2^i and ν_i, are varied until agreement is achieved.

The capabilities of this approach include the definition of the kinetic rate constants within time limits determined by the nature of the changes in line widths and peak positions and the chemical shift differences $\Delta\delta$ between the sites. For the cases discussed in the text, a value of $\Delta\delta \sim 200$ Hz [i.e., $\delta(E_pCd_2) - \delta(E_pCd_2S_p)$] defined lower limits for $k_3 \sim 500\ s^{-1}$ and $k_{-3} \sim 1000\ s^{-1}$ while $\Delta\delta \sim 20$ Hz [i.e., $\delta(E_pCdS_p) - \delta(E_pCd_2S_p)$] defined upper limits for $k_4 \sim 16\ s^{-1}$ and $k_{-4} \sim 12\ s^{-1}$. A further result of the line shape analysis was differentiating between two possible kinetic schemes. With the spectra in Figure 1 it was possible to eliminate a linear kinetic scheme including two enzyme–ligand complexes in which the first bound state converts to a second form; a linear scheme was not consistent with the spectra allowing all kinetic constants and ν_i to vary.

REFERENCES

Crothers, D. M., Cole, P. E., Hilbers, C. W., & Shulman, R. G. (1974) *J. Mol. Biol. 87*, 63–88.

Grassi, M., Mann, B. E., Pickup, B. T., & Spencer, C. M. (1986) *J. Magn. Reson. 69*, 92–99.

Johnston, E. R., Dellwo, M. J., & Hendrix, J. (1986) *J. Magn. Reson. 66*, 399–409.

McConnell, H. M. (1958) *J. Chem. Phys. 28*, 430–431.

Mendz, G. L., Robinson, G., & Kuchel, P. W. (1986) *J. Am. Chem. Soc. 108*, 169–173.

Perrin, C. L., & Gipe, R. K. (1984) *J. Am. Chem. Soc. 106*, 4036–4038.

Post, C. B., Ray, W. J., Jr., & Gorenstein, D. G. (1989) *Biochemistry 28*, 548–558.

Sandström, J. (1982) *Dynamic NMR Spectroscopy*, pp 6–29, Academic Press, London.

Vasavada, K. V., Kaplan, J., & Rao, B. D. N. (1980) *J. Magn. Reson. 41*, 467.